

Lawrence Berkeley National Laboratory

Recent Work

Title

Average Crystal Structure of the High- T_c Phase ($T_c \sim 111$ K) in the Sb-Pb-Bi-Sr-Ca-Cu-O System

Permalink

<https://escholarship.org/uc/item/1rs2j3w4>

Authors

Kijima, N.
Gronsky, R.

Publication Date

1990-12-01



Lawrence Berkeley Laboratory

UNIVERSITY OF CALIFORNIA

Materials & Chemical Sciences Division

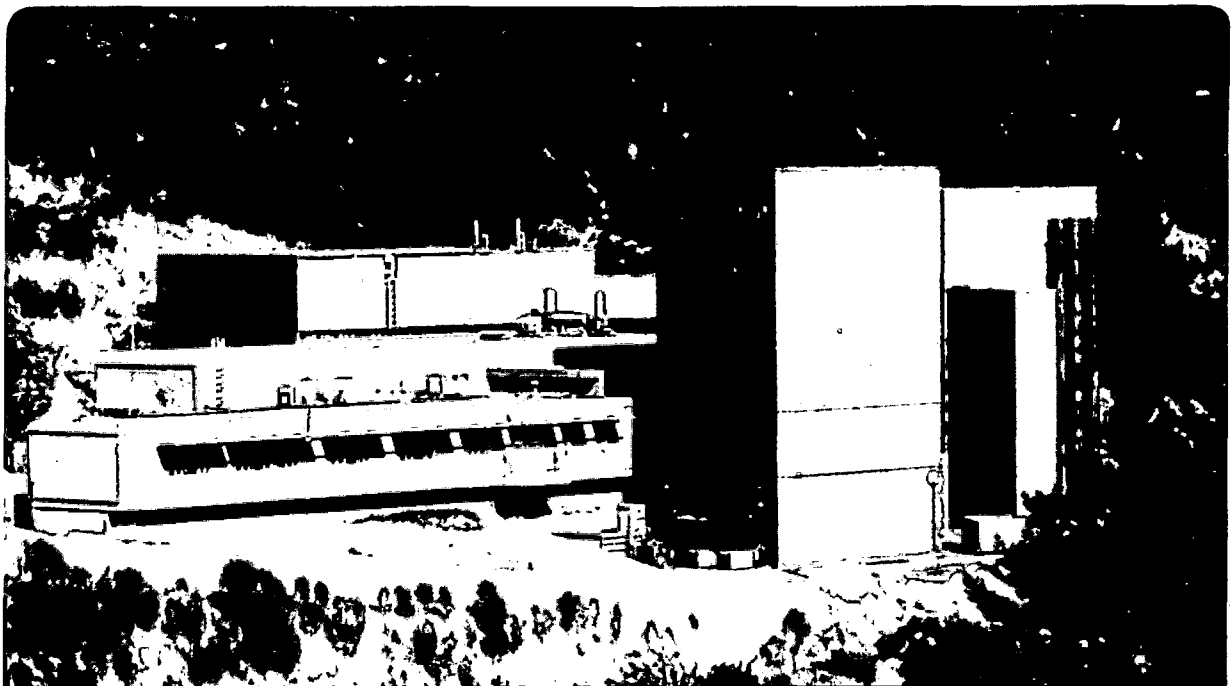
National Center for Electron Microscopy

Submitted to Applied Physics Letters

**Average Crystal Structure of the High- T_c Phase
($T_c \sim 111$ K) in the Sb-Pb-Bi-Sr-Ca-Cu-O System**

N. Kijima and R. Gronsky

December 1990



LOAN COPY
Circulates
for 2 weeks

Bldg. 50 Library.
Copy 2

LBL-30048

DISCLAIMER

This document was prepared as an account of work sponsored by the United States Government. While this document is believed to contain correct information, neither the United States Government nor any agency thereof, nor the Regents of the University of California, nor any of their employees, makes any warranty, express or implied, or assumes any legal responsibility for the accuracy, completeness, or usefulness of any information, apparatus, product, or process disclosed, or represents that its use would not infringe privately owned rights. Reference herein to any specific commercial product, process, or service by its trade name, trademark, manufacturer, or otherwise, does not necessarily constitute or imply its endorsement, recommendation, or favoring by the United States Government or any agency thereof, or the Regents of the University of California. The views and opinions of authors expressed herein do not necessarily state or reflect those of the United States Government or any agency thereof or the Regents of the University of California.

**Average Crystal Structure of the High- T_c Phase ($T_c \sim 111$ K)
in the SB-Pb-Bi-Sr-Ca-Cu-O System**

**Naoto Kijima and Ronald Gronsky
National Center for Electron Microscopy
Materials Sciences Division
Lawrence Berkeley Laboratory
University of California
Berkeley, California 94720**

December 1990

**Average Crystal Structure of the High- T_c Phase ($T_c \sim 111\text{K}$)
in the Sb-Pb-Bi-Sr-Ca-Cu-O System**

Naoto Kijima and Ronald Gronsky

*National Center for Electron Microscopy, Materials Sciences Division, Lawrence Berkeley
Laboratory, University of California, Berkeley, California 94720*

(Received)

The average crystal structure of the high- T_c phase ($T_c \sim 111\text{K}$) in the Sb-Pb-Bi-Sr-Ca-Cu-O system has been determined using transmission electron microscopy. The distance between the central Cu-O layer and the outer Cu-O layers of the high- T_c phase is slightly shorter than that of the high- T_c phase in the Bi-Sr-Ca-Cu-O and Pb-Bi-Sr-Ca-Cu-O systems due to the partial substitution of Sb for Ca between the Cu-O layers. When trivalent Sb substitutes for divalent Ca, oxygen atoms are also introduced to compensate the oxygen deficiency in the central Cu-O layer sandwiched by the two Ca/Sb layers.

Since the discovery of high- T_C superconductivity in the Bi-Sr-Ca-Cu-O system,¹ various dopants have been used to try to increase its critical temperature. It has been reported that the substitution of Sb and/or Pb for Bi in $\text{Bi}_2\text{Sr}_2\text{Ca}_2\text{Cu}_3\text{O}_x$ increases the endpoint critical temperature ($T_{C, end}$) to 132K.^{2, 3} However, Hongbao *et al.* have reported that this phase is so unstable that the $T_{C, end}$ decreases to 112K upon forming a stable phase after thermal cycling between 77K and room temperature.

In other manuscripts,^{4, 5} the superconducting properties, chemical composition and microstructure of the stable high- T_C phase ($T_C \sim 111\text{K}$) in the Sb-Pb-Bi-Sr-Ca-Cu-O system were described; the Sb-bearing superconducting phase has a 4K higher critical temperature than that in the Pb-Bi-Sr-Ca-Cu-O system. The average chemical composition of the high- T_C phase is 4.3%, 2.6%, 19.2%, 21.4%, 15.8% and 36.9% for Sb, Pb, Bi, Sr, Ca and Cu, respectively, and a summation of the Sb concentration and the Ca concentration is approximately the same for all the samples of this phase. The crystal structure of the high- T_C phase belongs to the superspace group $N_{1\bar{1}1}^{Bbmb}$, N_{111}^{Bb2b} , $P_{1\bar{1}1}^{Bbmb}$ or P_{111}^{Bb2b} with subcell lattice parameters $a=5.411(1)\text{\AA}$, $b=5.411(1)\text{\AA}$ and $c=37.22(6)\text{\AA}$, and the c -axis parameter is a slightly longer than that in the Pb-Bi-Sr-Ca-Cu-O system. The high- T_C phase also has a modulated structure with b -axis wavelengths 26.9Å and 36.1Å, the latter wavelength is also characteristic of the high- T_C phase in the Sb-Pb-Bi-Sr-Ca-Cu-O system. Stacking faults along the c -axis in the high- T_C phase are much less numerous than in the Bi-Sr-Ca-Cu-O system, but comparable to the Pb-Bi-Sr-Ca-Cu-O system. These results imply that Sb substitutes for Ca, and oxygen atoms are introduced to compensate the oxygen deficiency in the central Cu-O layer sandwiched by the two Ca layers in the crystal structure of the high- T_C phase.

In order to further clarify the effect of the Sb atoms on the crystal structure of the high- T_C phase, this detailed study of its crystal structure has been undertaken.

A sample with nominal composition $\text{Sb}_{0.10}\text{Pb}_{0.50}\text{Bi}_{1.40}\text{Sr}_{2.00}\text{Ca}_{2.00}\text{Cu}_{3.00}\text{O}_x$ was prepared by a solid-state reaction upon firing at 865°C for 504 hours in air as

described in another report.⁴ The fired specimen was then cut into small pieces, thinned, dimpled and ion-milled for transmission electron microscopy. Ion milling was carried out at 77K with argon ions accelerated at 3kV and the gun angle of 10 degrees. Transmission electron microscopy was carried out using an ARM-1000 high-resolution electron microscope operated at 800kV. The images taken by the microscope were processed by means of a Fourier filter using the image processing program SEMPER.⁶ Image simulations were also carried out with the image simulation code NCEMSS.⁷

Figure 1 shows a high-resolution transmission electron microscope image with the incident electron beam along the $[\bar{1}10]$ direction and the corresponding electron diffraction pattern. The observed region of the crystal consists of dominant layers of the high- T_C phase ($T_C \sim 111\text{K}$) and two stacking faults marked (S_1) and (S_2). Stacking fault S_2 has the same thickness as the c lattice parameter of the low- T_C phase ($T_C \sim 80\text{K}$), and stacking fault S_1 has its half thickness. Although two kinds of modulated structure in the high- T_C phase are observed on the (100) plane as shown in Figure 2, neither modulated structures nor satellite spots are observed in Fig.1. Therefore, it is possible to determine the average crystal structure of the high- T_C phase with a through-focus series of the transmission electron microscope images along the $[\bar{1}10]$ direction. The area marked (A), which doesn't include the stacking faults, was chosen to determine the crystal structure of the high- T_C phase.

As reported in another manuscript,⁵ the space group of the average crystal structure of the high- T_C phase in the Sb-Pb-Bi-Sr-Ca-Cu-O system is $Bbmb$ or $Bb2b$. Space group $Bbmb$ with higher symmetry than $Bb2b$ was assumed as an input structure to simulate the images. Debye-Waller temperature factors for most atoms in the high- T_C phase were fixed to the same values as those determined by the Rietveld analysis for the crystal structure of the high- T_C phase in the Pb-Bi-Sr-Ca-Cu-O system.⁸ The site occupancy of Sb at Ca sites and Pb at Bi sites was determined in conjunction with the results of the chemical composition obtained from energy dispersive X-ray spectroscopy.⁴

Figure 3 shows a through-focus series of the original images, processed images and simulated images of the crystal structure of the high- T_C phase. The images are closely matched with each other at the same defocus values. Table 1 shows the atomic parameters determined by the image simulation. The crystal structure of the high- T_C phase in the Sb-Pb-Bi-Sr-Ca-Cu-O system is close to that in the Bi-Sr-Ca-Cu-O⁹ and Pb-Bi-Sr-Ca-Cu-O⁸ systems; three Cu-O layers, two Ca(Sb) layers and two Sr-O layers are sandwiched between double Bi(Pb)-O layers. Each Ca(Sb) layer lies between two Cu-O layers, and each Sr-O layer is between the outer Cu-O layer and the Bi(Pb)-O layer.

The x coordinates of the atoms at 8l sites were determined from the images in Fig. 4, obtained with the incident electron beam along the b -axis. Dark dots corresponding to Bi(Pb) sites line up in pairs in the images because of the deviation of Bi(Pb) positions from $x=0.25$. This deviation contributes to the excitation of the diffraction spots with $h0l$ where $h=2n+1$ (n , integer) as shown in Fig. 4(a). If there were no deviation of Bi(Pb) along the a -axis, the symmetry of the average crystal structure would increase from $Bbmb$ to $I4/mmm$ because the a -axis lattice parameter is the same as the b -axis.

Since the high- T_C phase in the Sb-Pb-Bi-Sr-Ca-Cu-O system has two types of modulated structure as shown in Fig. 2, the calculated atomic coordinates represent the average positions of the atoms on the modulation waves. The deviations from the average atomic positions appear especially large in Bi(Pb)-O layers because the large dark dots corresponding to Bi(Pb) are elongated along the layers. We had to assume large values of Debye-Waller temperature factors for the atoms near the Bi(Pb)-O layers to absorb large positional deviations along the b -axis due to the modulated structures. Therefore, the deviations along the b -axis from the average atomic positions occur mainly near the Bi(Pb)-O layers to create the modulated structures in the high- T_C phase of the Sb-Pb-Bi-Sr-Ca-Cu-O system.

Table 2 shows the comparison of the distances between adjacent cation layers in the Bi-Sr-Ca-Cu-O, Pb-Bi-Sr-Ca-Cu-O and Sb-Pb-Bi-Sr-Ca-Cu-O systems. The distance

between the central Cu-O layer and the outer Cu-O layers in the high- T_c phase of the Sb-Pb-Bi-Sr-Ca-Cu-O system is slightly shorter than that of the Bi-Sr-Ca-Cu-O and Pb-Bi-Sr-Ca-Cu-O systems. When the smaller Sb^{3+} cation substitutes for the large Ca^{2+} cation, the Cu-O layers bordering the Ca(Sb) layer relax into this closer separation distance.

Also, because trivalent Sb occupies a fraction of the divalent Ca sites, more oxygen atoms have to be introduced into the Cu-O layers to compensate for the resulting charge imbalance. With a high resolution electron microscope, Hetherington et al.⁹ observed a 50 percent oxygen deficiency in the central Cu-O layer of the high- T_c phase in the Bi-Sr-Ca-Cu-O system. In the Sb-Pb-Bi-Sr-Ca-Cu-O system, however, there is no oxygen deficiency in the central Cu-O layer. Figure 5 shows the comparison between the simulated images in Fig. 3 and ones based upon the hypotheses that there is (1) no substitution of Sb for Ca, and (2) a 50% oxygen deficiency. A poor match at -12nm defocus between the processed image in Fig. 3 and the simulation with no Sb substitution is apparent from a detailed comparison of frames E in Fig. 3 and E in Fig. 5. Furthermore, at -28nm defocus the contrast in the central Cu-O layer (marked O_1) of the oxygen deficient model is brighter than the contrast in the outer Cu-O layers (marked O_{23}), and this is not seen in the processed image when frames G in Fig. 3 and K in Fig. 5 are compared. We therefore conclude that more oxygen atoms are introduced to make up for this oxygen deficiency as a result of the substitution of Sb for Ca, which affect the electronic state of the central Cu-O layer to increase the critical temperature from 107K to 111K.

The distance between two Bi(Pb)-O layers in the Pb-Bi-Sr-Ca-Cu-O and Sb-Pb-Bi-Sr-Ca-Cu-O systems is longer than that in the Bi-Sr-Ca-Cu-O system. The ionic radius of Pb^{2+} is slightly larger than that of Bi^{3+} , but the difference between the two is not big enough to explain the difference in the distance between two Bi(Pb)-O layers. Therefore, this difference may be due to the difference in the valence.

In conclusion, the crystal structure of the high- T_c phase in the Sb-Pb-Bi-Sr-Ca-Cu-O system is close to that in both the Bi-Sr-Ca-Cu-O and the Pb-Bi-Sr-Ca-Cu-O systems; three

Cu-O layers, two Ca(Sb) layers and two Sr-O layers are sandwiched between double Bi(Pb)-O layers. Each Ca(Sb) layer lies between two Cu-O layers, and each Sr-O layer lies between the outer Cu-O layer and the Bi(Pb) layer. The distance between the central Cu-O layer and the outer Cu-O layers in the high- T_c phase of the Sb-Pb-Bi-Sr-Ca-Cu-O system is slightly shorter than that of the Bi-Sr-Ca-Cu-O and Pb-Bi-Sr-Ca-Cu-O systems. Since the smaller Sb^{3+} cation substitutes for the large Ca^{2+} cation, the Cu-O layers separated by the Ca(Sb) layer relax into a shorter separation distance. Furthermore, when trivalent Sb occupies a fraction of the divalent Ca sites, more oxygen atoms than in the high- T_c phase of the Bi-Sr-Ca-Cu-O system are introduced into the central Cu-O layer to compensate for the resulting charge imbalance in the high- T_c phase of the Sb-Pb-Bi-Sr-Ca-Cu-O system. The compensation of the oxygen deficiency observed in the high- T_c phase of the Bi-Sr-Ca-Cu-O system affects the electronic state of the central Cu-O layer to increase the critical temperature from 107K to 111K.

We thank Mr. John Turner of the National Center for Electron Microscopy, LBL, for his assistance in image processing. This work was supported by the Director, Office of Energy Research, Office of Basic Energy Sciences, Materials Sciences Division, of the U.S. Department of Energy under Contract No. DE-AC03-76SF00098.

References

- ¹ H. Maeda, Y. Tanaka, M. Fukutomi, and T. Asano, *Jpn. J. Appl. Phys.* **27**, L209 (1988).
- ² L. Hongbao, C. Liezhao, Z. Ling, M. Zhigiang, L Xiaoxian, Y. Zhidong, X. Bai, M. Xianglei, Z. Guien, R. Yaozhong, C. Zhaojia, and Z. Yuheng, *Solid State Commun.* **69**, 867 (1989).
- ³ M. R. Chandrachood, I. S. Mulla, and A. P. B. Sinha, *Appl. Phys. Lett.* **55**, 1472 (1989).
- ⁴ N. Kijima, R. Gronsky, H. Endo, Y. Oguri, S. K. McKernan, and A. Zettl, unpublished.
- ⁵ N. Kijima, R. Gronsky, H. Endo, Y. Oguri, S. K. McKernan, and A. Zettl, unpublished.
- ⁶ W. O. Saxton, T. J. Pitt, and M. Horner, *Ultramicroscopy* **4**, 343 (1979).
- ⁷ R. Kilaas, in *Proceedings of the 45th Annual Meeting of the Electron Microscopy Society of America*, 66 (1987).
- ⁸ N. Kijima, H. Endo, J. Tsuchiya, A. Sumiyama, M. Mizuno, and Y. Oguri, *Jpn. J. Appl. Phys.* **28**, L787 (1989).
- ⁹ C. J. D. Hetherington, R. Ramesh, M. A. O'Keefe, R. Kilaas, G. Thomas, S. M. Green, and H. L. Luo, *Appl. Phys. Lett.* **53**, 1016 (1988).

Table 1. Atomic parameters of the crystal structure of the high- T_C phase in the Sb-Pb-Bi-Sr-Ca-Cu-O system. B is the isotropic temperature factor, and g is the site occupancy.

Atom	Site	x	y	z	$B/\text{\AA}^2$	g
Bi	8l	0.217	0.5	0.0440	4.0	0.88
Pb	8l	0.217	0.5	0.0440	4.0	0.12
Sr	8l	0.25	0.0	0.1158	3.0	1.0
Ca	8l	0.25	0.0	0.2057	1.3	0.80
Sb	8l	0.25	0.0	0.2057	1.3	0.20
Cu1	4f	0.25	0.5	0.2500	1.3	1.0
Cu2	8l	0.25	0.5	0.1613	1.3	1.0
O1	8h	0.0	0.25	0.2500	1.3	1.0
O2	8h	0.0	0.25	0.1643	1.3	1.0
O3	8h	0.5	0.25	0.1643	1.3	1.0
O4	8l	0.25	0.5	0.0990	5.0	1.0
O5	8l	0.217	0.0	0.0440	8.0	1.0

Table 2. Comparison of the distances between adjacent cation layers in the high- T_c phases of the three Bi-based systems. The distances between the layers were defined with the z coordinates of the cations.

Layers	Bi-Sr-Ca-Cu-O ^a	Pb-Bi-Sr-Ca-Cu-O ^b	Sb-Pb-Bi-Sr-Ca-Cu-O
Bi(Pb)-Bi(Pb)	2.88	3.15	3.28
Bi(Pb)-Sr	2.81	2.64	2.67
Sr-Cu2	1.65	1.69	1.69
Cu2-Ca(Sb)	1.67	1.69	1.65
Ca(Sb)-Cu1	1.69	1.67	1.65

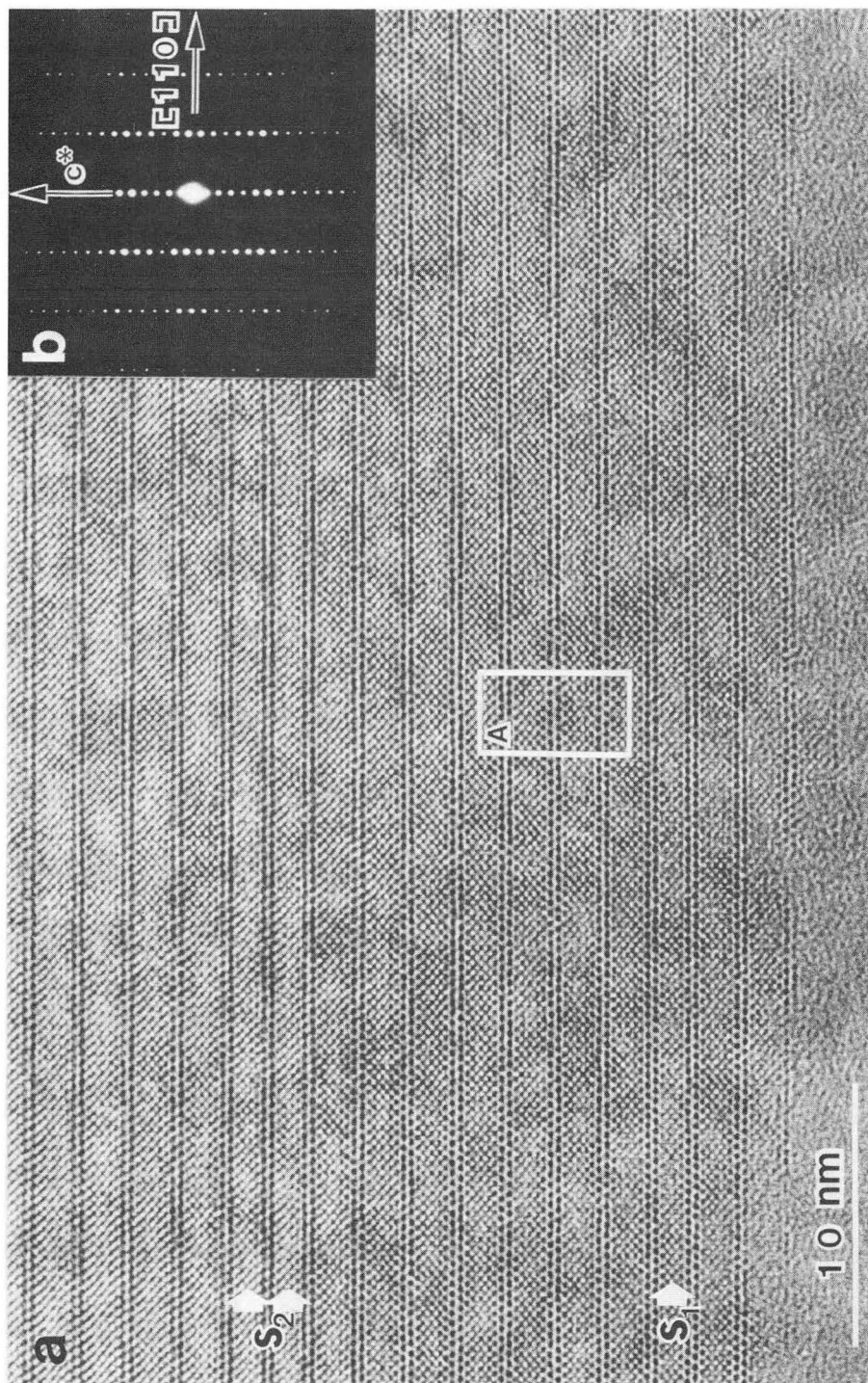
^aReference 9.

^bReference 8.

Figure Captions

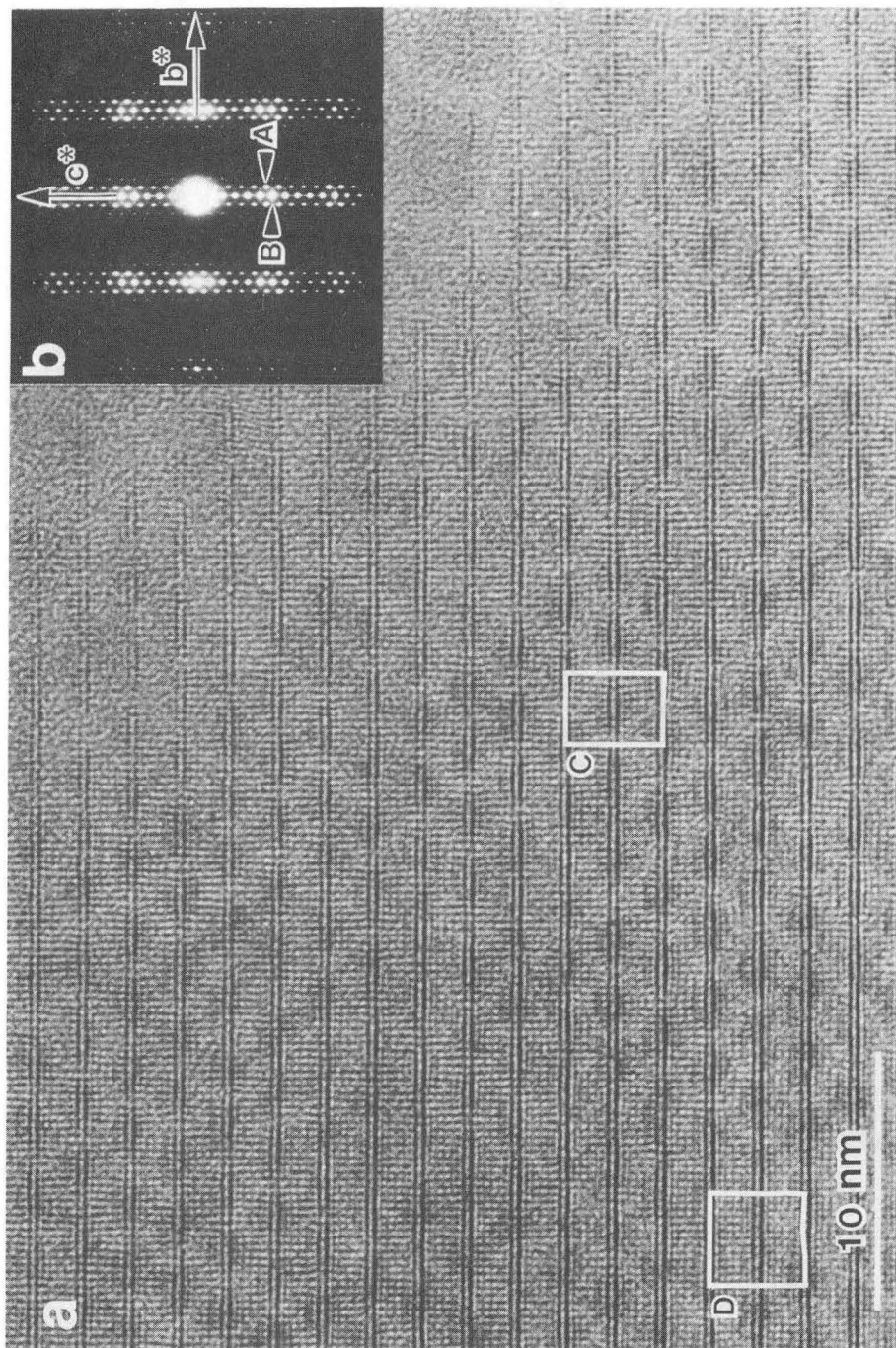
- Fig. 1. Phase contrast high-resolution transmission electron microscope image (a) and corresponding selected area diffraction pattern (b) of the high- T_C phase in the Sb-Pb-Bi-Sr-Ca-Cu-O system with the incident electron beam along the $[\bar{1}10]$ direction. Note that there are two types of stacking faults marked (S_1) and (S_2). Stacking fault S_2 has the same thickness as the c lattice parameter of the low- T_C phase ($T_C \sim 80\text{K}$), and stacking fault S_1 has its half thickness. The area marked (A) was chosen to determine the crystal structure of the high- T_C phase.
- Fig. 2. Phase contrast high-resolution transmission electron microscope image (a) and corresponding selected area diffraction pattern (b) of the high- T_C phase in the Sb-Pb-Bi-Sr-Ca-Cu-O system with the incident electron beam along the a -axis. Note that there are two types of modulated structure marked (C) and (D) in the image, and corresponding satellite spots marked (A) and (B) in the diffraction pattern. The b -axis components of wave vectors of modulated structures marked (C) and (D) have magnitudes of 26.9\AA and 36.1\AA , respectively.
- Fig. 3. Through-focus series of phase contrast high-resolution transmission electron microscope images (A)~(D) with objective lens defoci -12nm ~ -36nm , corresponding processed images (E)~(H) by means of Fourier filtering, and simulated images (I)~(L) using the atomic parameters in Table 1. The incident electron beam is along the $[\bar{1}10]$ direction. The foil thickness is 6 nm . The calculated area is the same as the part marked (A) in Figure 1.
- Fig. 4. Phase contrast high-resolution transmission electron microscope image (b), corresponding selected area diffraction pattern (a), processed image (c), and simulated image (d) of the high- T_C phase in the Sb-Pb-Bi-Sr-Ca-Cu-O system with the incident electron beam along the b -axis. Note that dark dots corresponding to Bi(Pb) atom positions line up in pairs.

Fig. 5 Simulated images of the high- T_c phase from the $[\bar{1}10]$ direction. Images (A)~(D) are based on the crystal structure with the atomic parameters in Table 1. Images (E)~(H) are based on the hypothesis that Sb doesn't substitute for Ca at all. Images (I)~(L) are based on the hypothesis that there is 50% oxygen deficiency in the central Cu-O layer. The foil thickness and the objective defoci are 60 nm and -12nm~-36nm, respectively.



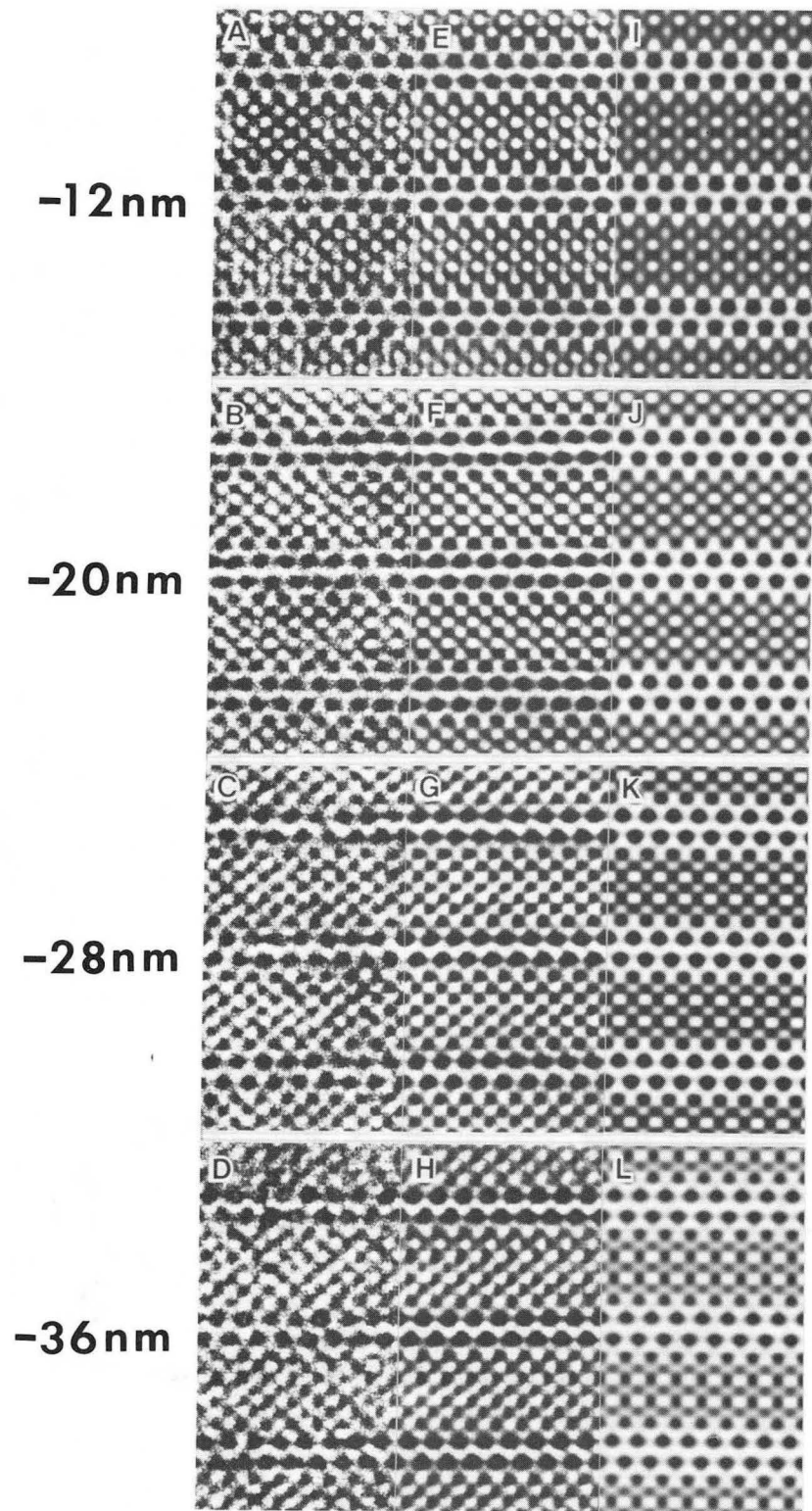
XBB 912-914

Fig. 1.



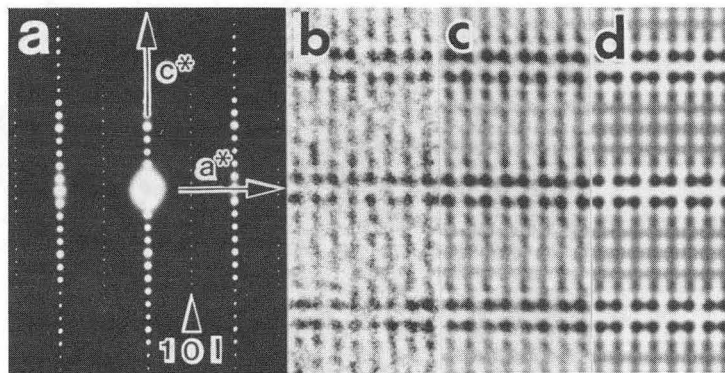
XBB 912-915

Fig. 2.



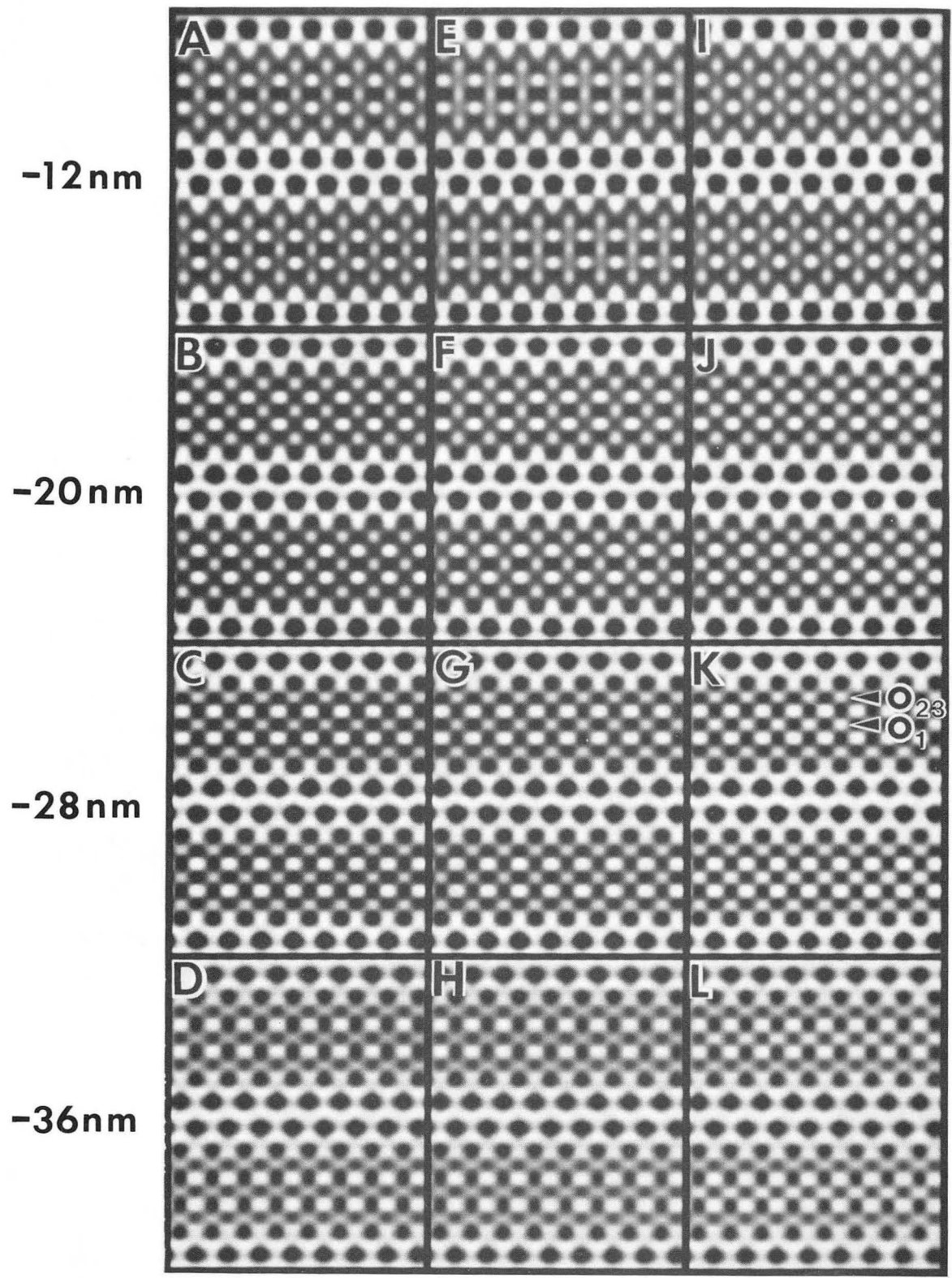
XBB 912-916

Fig. 3.



XBB 912-917

Fig. 4.



XBB 912-918

Fig. 5.

LAWRENCE BERKELEY LABORATORY
UNIVERSITY OF CALIFORNIA
INFORMATION RESOURCES DEPARTMENT
BERKELEY, CALIFORNIA 94720